

DIFFUSE OPTICAL TOMOGRAPHY BY SIMULATED ANNEALING VIA A SPIN HAMILTONIAN

YU JIANG¹, MANABU MACHIDA², AND NORIKAZU TODOROKI³

ABSTRACT. The inverse problem of diffuse optical tomography is solved by the Markov-chain Monte Carlo. The Metropolis algorithm or single-component Metropolis-Hastings algorithm is used. The value of the unknown parameter is discretized and a spin Hamiltonian is introduced in the cost function. Then an initial random spin configuration is brought to a converged configuration by simulated annealing.

1. INTRODUCTION

Diffuse optical tomography is an imaging modality which uses near-infrared light [7, 17]. To obtain reconstructed images of diffuse optical tomography, inverse problems of determining coefficients of the diffusion equation from boundary measurements are solved. For these inverse problems in diffuse optical tomography, direct approaches such as the use of the Born approximation and iterative methods such as the conjugate gradient method and damped Gauss-Newton method are commonly used [1, 3]. In the direct approach, the inversion by singular value decomposition corresponds to the L^2 regularization. Although different penalty terms can be employed in iterative methods, the calculation is trapped by local minima unless a good initial guess is given. Statistical approaches have been developed in diffuse optical tomography [2, 16]. To estimate parameters in coefficients of the diffusion equation or the radiative transport equation, which is approximated to the diffusion equation at large scales, the Metropolis-Hastings Monte Carlo algorithm was used [5, 12, 9]. However, only a few unknown parameters can be determined by the naive use of the Metropolis-Hastings Markov-chain Monte Carlo method.

In this paper, we propose a new way of using the Markov-chain Monte Carlo for diffuse optical tomography. We solve the inverse problem of determining the absorption coefficient of the diffusion equation by the single-component Metropolis-Hastings algorithm and simulated annealing after the cost function is turned into a spin Hamiltonian. The penalty term used in the algorithm is not restricted to the 2-norm. In this paper we use the 1-norm.

¹SCHOOL OF MATHEMATICS, SHANGHAI UNIVERSITY OF FINANCE AND ECONOMICS, SHANGHAI 200433, P.R. CHINA

²INSTITUTE FOR MEDICAL PHOTONICS RESEARCH, HAMAMATSU UNIVERSITY SCHOOL OF MEDICINE, HAMAMATSU 431-3192, JAPAN

³DEPARTMENT OF PHYSICS, CHIBA INSTITUTE OF TECHNOLOGY, CHIBA 275-0023, JAPAN
E-mail addresses: jiang.yu@mail.shufe.edu.cn, machida@hama-med.ac.jp, todoroki.norikazu@p.chibakoudai.jp.

Date: October 13, 2021.

2. DIFFUSION EQUATION

We consider diffuse optical tomography in the half space Ω in \mathbb{R}^2 , i.e., $\Omega = \{x \in \mathbb{R}^2; x_1 \in \mathbb{R}, 0 < x_2 < \infty\}$. Let $\partial\Omega$ be the boundary of Ω , which is the x_1 -axis. We assume that Ω is occupied by biological tissue and $\mathbb{R}^2 \setminus \bar{\Omega}$ is vacuum. Let u be the photon density of near-infrared light. Light propagation in Ω is governed by the following diffusion equation for $u(x)$ ($x \in \Omega$).

$$\begin{cases} -D_0 \Delta u + \mu_a u = f, & x \in \Omega, \\ -D_0 \frac{\partial}{\partial y} u + \frac{1}{\zeta} u = 0, & x \in \partial\Omega, \end{cases} \quad (2.1)$$

where the diffusion coefficient $D_0 > 0$ is assumed to be a constant, $\zeta > 0$ is a constant, and the absorption $\mu_a(x) \geq 0$ varies in space. The incident beam $f(x)$ is assumed to be a pencil beam given by $f(x) = g_0 \delta(x - x_s^{(p)})$, where $g_0 > 0$ is a constant and $x_s^{(p)} = (x_{s1}^{(p)}, 0^+)$ is the position of the source of the p th source-detector pair ($p = 1, 2, \dots, M_{\text{SD}}$). Light is detected on the boundary at $x_d^{(p)} = (x_{d1}^{(p)}, 0)$.

We choose a region of interest Ω_{ROI} in Ω . We suppose $\mu_a(x) = \bar{\mu}_a$, $x \in \bar{\Omega} \setminus \Omega_{\text{ROI}}$, where $\bar{\mu}_a$ is a nonnegative constant. Let us write $\mu_a(x)$ as

$$\mu_a(x) = \bar{\mu}_a + \delta\mu_a(x), \quad x \in \Omega_{\text{ROI}},$$

where we assume $\delta\mu_a \in [0, \delta\mu_a^{(\max)}]$ with a constant $\delta\mu_a^{(\max)} > 0$. Let M be an even integer. We introduce a *spin* variable of discrete values as

$$S(x) = 0, \pm 1, \pm 2, \dots, \pm \frac{M}{2}, \quad x \in \Omega_{\text{ROI}},$$

and express $\delta\mu_a(x)$ as

$$\delta\mu_a(x) = \delta\mu_a^{(\max)} \left(\frac{S(x)}{M} + \frac{1}{2} \right).$$

Thus $\delta\mu_a$ is discretized in $[0, \mu_a^{(\max)}]$ by $M + 1$ values.

3. RYTOV APPROXIMATION

Let $u_0(x)$ be the solution to (2.1) in the case of $\delta\mu_a \equiv 0$. Then $u_0(x) = g_0 G(x, x_s^{(p)})$, where $G(x, y)$ is the Green's function, which satisfies (2.1) with the source term $f(x) = \delta(x - y)$. The Green's function is obtained as

$$G(x, y) = \frac{1}{2\pi D_0} \int_0^\infty \frac{\cos(q(x_1 - y_1))}{\lambda} \left(e^{-\lambda|x_2 - y_2|} + \frac{\ell\lambda - 1}{\ell\lambda + 1} e^{-\lambda(x_2 + y_2)} \right) dq, \quad (3.1)$$

where $\ell = \zeta D_0$ and $\lambda = \lambda(q) = \sqrt{\frac{\bar{\mu}_a}{D_0} + q^2}$. We note that $\|G(x, \cdot)\|_{L^1(\Omega)} < \infty$ and $\|G(x, \cdot)\|_{L^\infty(\Omega)} < \infty$ for any $x \in \Omega$.

The solution $u(x)$ satisfies the following identity.

$$u(x) = u_0(x) - \int_\Omega G(x, y) \delta\mu_a(y) u(y) dy.$$

The n th Born approximation u_n is given by $u_n = \sum_{k=0}^n v_k$, where $v_{k+1}(x) = -\int_\Omega G(x, y) \delta\mu_a(y) v_k(y) dy$ ($k = 0, 1, \dots$) and $v_0(x) = u_0(x)$. When the perturbation $\delta\mu_a$ is small, the Born series converges and $u = \lim_{n \rightarrow \infty} u_n$. In particular for nonnegative $\delta\mu_a$, a concise proof of the convergence is known under the condition

$0 \leq \delta\mu_a(x) \leq \bar{\mu}_a$ for any $x \in \Omega$ [13]. Let us define the first and second Rytov approximations u_R, u_{R2} as

$$u_R = u_0 e^{v_1/u_0}, \quad u_{R2} = u_0 e^{v_1/u_0} \exp \left[\frac{v_2}{u_0} - \frac{1}{2} \left(\frac{v_1}{u_0} \right)^2 \right].$$

Lemma 3.1. *Suppose $\|\delta\mu_a\|_{L^\infty(\Omega)}$ is sufficiently small. Then there exists a positive constant C_1 such that*

$$\|u - u_R\|_{L^\infty(\Omega)} \leq C_1 \|\delta\mu_a\|_{L^\infty(\Omega)} \|u_0\|_{L^\infty(\Omega)}.$$

Proof. We have

$$u(x) - u_R(x) = u_0(x) \left(1 - e^{v_1/u_0} \right) - \int_{\Omega} G(x, y) \delta\mu_a(y) u_R(y) dy - \int_{\Omega} G(x, y) \delta\mu_a(y) (u(y) - u_R(y)) dy.$$

Therefore for sufficiently small $\|\delta\mu_a\|_{L^\infty(\Omega)}$, we obtain

$$\|u - u_R\|_{L^\infty(\Omega)} \leq C'_1 \|\delta\mu_a\|_{L^\infty(\Omega)} \|u_0\|_{L^\infty(\Omega)} + C'_1 \|\delta\mu_a\|_{L^\infty(\Omega)} \|u - u_R\|_{L^\infty(\Omega)},$$

where C'_1 is a positive constant. By moving the last term on the right-hand side to the left-hand side, we complete the proof. \square

The outgoing light is detected at $x_d^{(p)} \in \partial\Omega$. Let us introduce the data $\phi^{(p)}$ as

$$\phi^{(p)} = \ln \frac{u_0(x_d^{(p)})}{u(x_d^{(p)})}.$$

In the first Rytov approximation we have $\phi^{(p)} \approx \phi_{R2}^{(p)} \approx \phi_R^{(p)}$, where $\phi_R^{(p)} = -\frac{v_1(x_d^{(p)})}{u_0(x_d^{(p)})}$ and

$$\phi_{R2}^{(p)} = -\frac{v_1(x_d^{(p)})}{u_0(x_d^{(p)})} + \frac{1}{2} \left(\frac{v_1(x_d^{(p)})}{u_0(x_d^{(p)})} \right)^2 - \frac{v_2(x_d^{(p)})}{u_0(x_d^{(p)})}.$$

Lemma 3.2. *We assume that $\|\delta\mu_a\|_{L^\infty(\Omega)}$ is sufficiently small. Then there exists a positive constant C_2 such that*

$$|\phi^{(p)}| \leq \ln(1 + C_2 \|\delta\mu_a\|_{L^\infty(\Omega)}).$$

Proof. Note that u_0, u_R are positive. Using Lemma 3.1, we have

$$|\phi^{(p)}| = \left| \ln \left(\frac{u - u_R}{u_0} + \frac{u_R}{u_0} \right) \right| \leq \ln \left(\frac{C_1 \|\delta\mu_a\|_{L^\infty(\Omega)} \|u_0\|_{L^\infty(\Omega)}}{u_0} + e^{v_1/u_0} \right).$$

Then the lemma is proved for sufficiently small $\|\delta\mu_a\|_{L^\infty(\Omega)}$. \square

As is done in most numerical approaches, we discretize space. Let us divide the region of interest Ω_{ROI} into cells $\omega_i \subset \Omega$ ($i = 1, \dots, N$) such that $\Omega_{\text{ROI}} = \bigcup_{i=1}^N \omega_i$ and $\omega_{i_1} \cap \omega_{i_2} = \emptyset$ if $i_1 \neq i_2$. Let $|\omega|$ denote the area (volume) of subdomains ω_i . We have $N > M_{\text{SD}}$ as is seen below, and the inverse problem is underdetermined. We introduce

$$\delta\mu_a(y_i) = \delta\mu_a^{(\max)} \left(\frac{S_i}{M} + \frac{1}{2} \right), \quad S_i = 0, \pm 1, \pm 2, \dots, \pm \frac{M}{2}, \quad i = 1, \dots, N.$$

Let us define

$$K_{p,i} = \delta\mu_a^{(\max)} |\omega| \frac{G(x_d^{(p)}, y_i) G(y_i, x_s^{(p)})}{G(x_d^{(p)}, x_s^{(p)})},$$

where $y_i \in \omega_i$ is a representative point in ω_i . Assuming that ω_i is small, we can write

$$\phi^{(p)} \approx \phi_{R2}^{(p)} \approx \widetilde{\phi_{R2}^{(p)}},$$

where

$$\begin{aligned} \widetilde{\phi_{R2}^{(p)}} &= \sum_{i=1}^N K_{p,i} \left(\frac{S_i}{M} + \frac{1}{2} \right) + \frac{1}{2} \sum_{i_1=1}^N \sum_{i_2=1}^N K_{p,i_1} K_{p,i_2} \left(\frac{S_{i_1}}{M} + \frac{1}{2} \right) \left(\frac{S_{i_2}}{M} + \frac{1}{2} \right) \\ &\quad - |\omega|^2 \sum_{i_1=1}^N \sum_{i_2=1}^N \frac{G(x_d^{(p)}, y_{i_1}) \delta \mu_a(y_{i_1}) G(y_{i_1}, y_{i_2}) \delta \mu_a(y_{i_2}) G(y_{i_2}, x_s^{(p)})}{G(x_d^{(p)}, x_s^{(p)})}. \end{aligned}$$

4. SPIN HAMILTONIAN

We let $\Phi^{(p)}$ denote the experimentally obtained data corresponding to $\phi^{(p)}$. Let $S = (S_i) \in \mathbb{R}^N$ denote the spin configuration. We will look for S^* which minimizes the following cost function $\Psi(S)$.

$$\Psi(S) = \frac{1}{2} \sum_{p=1}^{M_{SD}} \left| \Phi^{(p)} - \widetilde{\phi_{R2}^{(p)}} \right|^2 + \alpha \sum_{i=1}^N |S_i - S_i^{(0)}|,$$

where $\alpha > 0$ is the regularization parameter and $(S_i^{(0)}) \in \mathbb{R}^N$ is an initial guess, which we set $S_i^{(0)} = -M/2$ ($i = 1, \dots, N$).

Theorem 4.1. *Choose arbitrary p, i_1, i_2 ($p = 1, \dots, M_{SD}$, $i_1, i_2 = 1, \dots, N$). Consider*

$$g_1 = K_{p,i_1} K_{p,i_2}, \quad g_2 = g_1 - 2 \left(\delta \mu_a^{(\max)} \right)^2 |\omega|^2 \frac{G(x_d^{(p)}, y_{i_1}) G(y_{i_1}, y_{i_2}) G(y_{i_2}, x_s^{(p)})}{G(x_d^{(p)}, x_s^{(p)})}.$$

Then $|g_1| \geq |\phi^{(p)} g_2|$ for sufficiently small $\|\delta \mu_a\|_{L^\infty(\Omega)}$.

Proof. Recall that $|\phi^{(p)}| \rightarrow 0$ as $\|\delta \mu_a\|_{L^\infty(\Omega)} \rightarrow 0$ according to Lemma 3.2. We have

$$\left| \phi^{(p)} g_2 \right| = |g_1| \left| \phi^{(p)} \frac{g_2}{g_1} \right| = |g_1| \left| \phi^{(p)} \right| \left| 1 - 2 \frac{G(x_d^{(p)}, x_s^{(p)}) G(y_{i_1}, y_{i_2})}{G(x_d^{(p)}, y_{i_2}) G(y_{i_1}, x_s^{(p)})} \right| \leq C |g_1|,$$

where nonnegative constant C is less than 1. \square

Then by neglecting g_2 , we have $\Psi = \mathcal{H}(S) + \text{const.}$, where only the first term on the right-hand side depends on S_i . The Hamiltonian $\mathcal{H}(S)$ is given by

$$\mathcal{H}(S) = - \sum_{i=1}^N \sum_{j=1}^N J_{ij} S_i S_j - \sum_{i=1}^N h_i S_i, \quad (4.1)$$

where

$$J_{ij} = \frac{-1}{2M^2} \sum_{p=1}^{M_{SD}} K_{p,i} K_{p,j}, \quad h_i = M \sum_{j=1}^N J_{ij} + \frac{1}{M} \left(\sum_{p=1}^{M_{SD}} \Phi^{(p)} K_{p,i} - \alpha \right).$$

The spin interactions are symmetric: $J_{ij} = J_{ji}$. We note that the modulus $|h_i|$ of the magnetic field increases as the hyperparameter α in the regularization term increases and the spin Hamiltonian has a unique ground state ($S^* = S^{(0)}$) for sufficiently large α .

Thus our optical tomography is reformulated as the problem of searching the ground state of $\mathcal{H}(S)$, i.e., the spin configuration $S^* = \arg \min_S \mathcal{H}(S)$.

5. SIMULATED ANNEALING

Let T be temperature. The simulated annealing finds the ground state S^* of $\mathcal{H}(S)$ in (4.1) by gradually decreasing temperature from T_{high} to T_{low} .

The partition function Z is given by $Z = \sum_{\{S_i\}} e^{-\beta \mathcal{H}}$, where $\beta = 1/T$ is the inverse temperature. Here, we used the notation $\sum_{\{S_i\}} = \sum_{S_1} \cdots \sum_{S_N}$. We treat $\{S_i\} = \{S_1, S_2, \dots, S_N\}$ as random variables. We give the probability density function $\pi(S)$ as the Boltzmann distribution given by

$$\pi(S) = \frac{e^{-\beta \mathcal{H}(S)}}{Z}. \quad (5.1)$$

We see that $\pi(S)$ is large if $\mathcal{H}(S)$ is small. When the temperature is sufficiently low, i.e., β is large, $\pi(S^*)$ becomes significantly larger than the probability of other configurations S .

Although calculating the denominator Z on the right-hand side of (5.1) is difficult, we can find S^* by using the Metropolis algorithm [14, 11]. The proposal distribution $q(S'_i|S)$ is given for each spin, say the i th spin, and the value of S'_i is generated with equal probability. We note that

$$\frac{\pi(S')}{\pi(S)} = e^{\beta(\mathcal{H}(S) - \mathcal{H}(S'))} = \exp \left[\beta \left(J_{ii} (S_i'^2 - S_i^2) + \left(2 \sum_{\substack{j=1 \\ j \neq i}}^N J_{ij} S_j + h_i \right) (S'_i - S_i) \right) \right].$$

The Metropolis algorithm or single-component Metropolis-Hastings algorithm is known to be effective [8], whereas the standard Metropolis-Hastings algorithm does not work in high dimensions with many unknown parameters [4, 10]. The algorithm is summarized as the following six steps.

- (1) Start with a small $\beta = 1/T_{\text{high}} > 0$. Give $(S_i) \in \mathbb{R}^N$ randomly as an initial guess. Then set $i = 1$.
- (2) Compute $h_{\text{eff},i} = 2 \sum_{j=1, (j \neq i)}^N J_{ij} S_j + h_i$.
- (3) Calculate $w = -\beta [h_{\text{eff},i} (S'_i - S_i) + J_{ii} (S_i'^2 - S_i^2)]$, where $S'_i \sim q(\cdot|S)$ is randomly chosen.
- (4) Set $S_i = S'_i$ if $w \leq 0$. Otherwise put $S_i = S'_i$ with probability e^{-w} .
- (5) Set $i = 1$ if $i = N$. Otherwise set $i = i+1$. Return to Step 2. After repeating several loops from Step 2 to Step 5 until the initial large fluctuation ceases, proceed to Step 6.
- (6) Decrease temperature and go to Step 2. If the temperature reaches T_{low} , finish the iteration.

6. NUMERICAL TEST

We use 16 sources $(x_{s1}^{(p)} = \pm 2, \pm 6, \dots, \pm 30 [\text{mm}])$ and 15 detectors $(x_{d1}^{(p)} = 0, \pm 4, \pm 8, \dots, \pm 28 [\text{mm}])$, which results in $M_{\text{SD}} = 240$ source-detector pairs. We compute the forward data $\Phi^{(p)}$ ($p = 1, \dots, M_{\text{SD}}$) by the finite-difference scheme. We added 3% Gaussian noise to $u(x_d^{(p)})$ and $u_0(x_d^{(p)})$. We set $\bar{\mu}_a = 0.02 \text{ mm}^{-1}$, $\mu'_s = 1.0 \text{ mm}^{-1}$, and the refractive index $n = 1.37$. We note that $D_0 = \frac{1}{3(\mu_a + \mu'_s)} =$

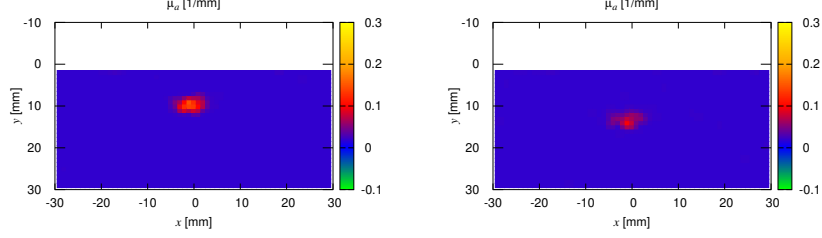


FIGURE 1. (Left) One absorber at the depth 10 mm. (Right) One absorber at a deeper position at $y = 15$ mm.

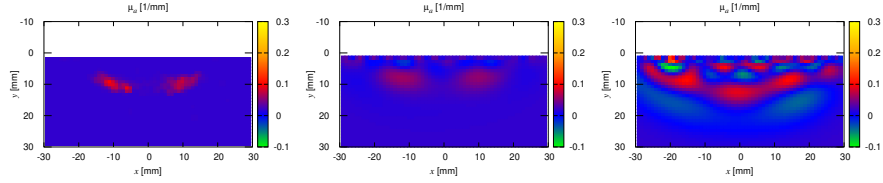


FIGURE 2. Two absorbers with separation 20 mm. (Left) The proposed method. (Middle) The reconstruction by the truncated SVD with 52 singular values. (Right) The reconstruction by the truncated SVD with 80 singular values.

0.33 mm. Inside the disk, $\delta\mu_a = 0.2 \text{ mm}^{-1}$. Assuming the diffuse surface reflection, we obtain $\zeta = 2 \frac{1+r_d}{1-r_d}$, where $r_d = -1.4399n^{-2} + 0.7099n^{-1} + 0.6681 + 0.0636n$ [6]. When calculating the Green's function, the numerical integration in (3.1) can be done by the double-exponential formula [15]. We take $(2N_x + 1)N_y = 1830$ cells ($N_x = 30$, $N_y = 30$) of the area $|\omega| = h^2$ ($h = 1$ mm). Moreover, the following parameter values were used for simulated annealing: $\alpha = 0.01$, $T_{\text{high}} = 10^{-5}$, $T_{\text{low}} = 10^{-10}$, $M = 256$.

Figures 1 and 2 show reconstructed images. In Fig. 1, a disk target of radius 2.5 mm was placed at the depth (Left) 10 mm and (Right) 15 mm, that is, the x and y coordinates of the disk center are $x = 0$ mm, and $y = 10$ mm or 15 mm. As is expected, the reconstruction at a deeper position is more difficult. Next we consider two disks of radius 2.5 mm. The centers of the disks are placed at $(x, y) = (\pm 10 \text{ mm}, 10 \text{ mm})$. For comparison, we also used the truncated SVD. Figures 2 (Left) shows the reconstruction by the proposed scheme using the same parameters described above for Fig. 1. Reconstructions from the truncated SVD are presented in Fig. 2 with (Middle) 52 largest singular values and (Right) 80 largest singular values, respectively. Using the truncated SVD, it is difficult to see a clear separation between the two targets.

7. CONCLUDING REMARKS

We have developed a statistical approach of diffuse optical tomography using the Metropolis algorithm of the Monte Carlo method. By the introduction of spin, the

forward problem needs to be solved only once before the Monte Carlo calculation begins.

For linearized inverse problems, the truncated singular value decomposition (SVD) is often used [1, 3]. Although the truncated SVD has a filtering property similar to the Tikhonov regularization, the penalty term of the proposed method is not restricted to the 2-norm. In this paper, the 1-norm was used. This might explain the difference of the quality of reconstruction in Fig. 2. Another advantage of our method is that it is feasible to use a priori information and set the lower and upper bounds of $\delta\mu_a$, whereas the reconstructed $\delta\mu_a$ by the truncated SVD is unbounded. This feature is reflected in the difference between the proposed method and SVD in Fig. 2.

Moreover the linearization in this paper is not essential. It is possible to take nonlinear terms in the Born and Rytov series into account. Then the spin Hamiltonian acquires additional terms for multi-body spin interactions.

ACKNOWLEDGEMENT

YJ is supported by the National Natural Science Foundation of China (No. 11971121). MM is supported by Grant-in-Aid for Scientific Research (17K05572, 17H02081, 18K03438) of JSPS and by HUSM Grant-in-Aid. NT is supported by Grant-in-Aid for Scientific Research (16K05418) of JSPS.

REFERENCES

- [1] S. R. Arridge. Optical tomography in medical imaging. *Inverse Problems*, 15:R41–R93, 1999.
- [2] S. R. Arridge, J. P. Kaipio, V. Kolehmainen, M. Schweiger, E. Somersalo, T. Tarvainen, and M. Vauhkonen. Approximation errors and model reduction with an application in optical diffusion tomography. *Inverse Problems*, 22:175–195, 2006.
- [3] S. R. Arridge and J. C. Schotland. Optical tomography: forward and inverse problems. *Inverse Problems*, 25:123010, 2009.
- [4] S.-K. Au and J. L. Beck. Estimation of small failure probabilities in high dimensions by subset simulation. *Probabilistic Engineering Mechanics*, 16:263–277, 2001.
- [5] G. Bal, I. Langmore, and Y. Marzouk. Bayesian inverse problems with monte carlo forward models. *Inv. Probl. Imag.*, 7:81–105, 2013.
- [6] W. G. Egan and T. W. Hilgeman. *Optical Properties of Inhomogeneous Materials*. Academic Press, New York, 1979.
- [7] A. P. Gibson, J. C. Hebden, and S. R. Arridge. Recent advances in diffuse optical imaging. *Phys. Med. Biol.*, 50:R1–R43, 2005.
- [8] W. R. Gilks, S. Richardson, and D. J. Spiegelhalter. *Markov Chain Monte Carlo in Practice*. Chapman and Hall, London, 1996.
- [9] Y. Jiang, Y. Hoshi, M. Machida, and G. Nakamura. A hybrid inversion scheme combining markov chain monte carlo and iterative methods for determining optical properties of random media. *Appl. Sci.*, 9:3500, 2019.
- [10] L. S. Katafygiotis and K. M. Zuev. Geometric insight into the challenges of solving high-dimensional reliability problems. *Probabilistic Engineering Mechanics*, 23:208–218, 2008.
- [11] D. P. Landau and K. Binder. *A Guide to Monte Carlo Simulations in Statistical Physics*. Cambridge University Press, London, 2000.
- [12] I. Langmore, A. B. Davis, and G. Bal. Multipixel retrieval of structural and optical parameters in a 2-d scene with a path-recycling monte carlo forward model and a new bayesian inference engine. *IEEE Trans. Geosci. Remote Sens.*, 51:2903–2919, 2013.
- [13] V. A. Markel and J. C. Schotland. On the convergence of the born series in optical tomography with diffuse light. *Inverse Problems*, 23:1445–1465, 2007.
- [14] N. Metropolis, A. W. Rosenbluth, M. N. Rosenbluth, A. H. Teller, and E. Teller. Equation of state calculations by fast computing machines. *J. Chem. Phys.*, 21:1087–1092, 1953.

- [15] T. Ooura and M. Mori. The double exponential formula for oscillatory functions over the half infinite interval. *J. Comput. Appl. Math.*, 38:353–360, 1991.
- [16] T. Shimokawa, T. Kosaka, O. Yamashita, N. Hiroe, T. Amita, Y. Inoue, and M. Sato. Hierarchical bayesian estimation improves depth accuracy and spatial resolution of diffuse optical tomography. *Opt. Exp.*, 20:20427–20446, 2012.
- [17] Y. Yamada and S. Okawa. Diffuse optical tomography: Present status and its future. *Opt. Rev.*, 21:185–205, 2014.